CRYSTAL GROWTH & DESIGN

pubs.acs.org/crystal

Article

Inhibition of the Antibiotic Activity of Cephalosporines by Co-Crystallization with Thymol

Published as part of a Crystal Growth and Design joint virtual special issue on Crystallizing the Role of Solid-State Form in Drug Delivery

Cecilia Fiore, Alessandra Baraghini, Oleksii Shemchuk, Vittorio Sambri,* Manuela Morotti, Fabrizia Grepioni, and Dario Braga*

Cite This: https://doi.org/10.1021/acs.cgd.1c01435

Read Online

ACCESS | Metrics & More | Article Recommendations | Supporting Information

ABSTRACT: Three structurally similar antibiotics of the cephalosporin (CEPH) class, namely, cephalexin (CPX), cephradine (CFD), and cefaclor (CFC), have been co-crystallized with thymol (THY) via different preparation techniques, yielding the hydrated co-crystals CPX·THY·2.5H_2O form I and form II, CFD·THY·2.5H_2O, and CFC·THY·4H_2O. All co-crystals were structurally characterized by single crystal and/or powder X-ray diffraction. In all co-crystals, except in the case of the elusive metastable form I of CPX·THY·2.5H_2O, the CEPH molecules interact with thymol only via water bridges; i.e., there is no direct hydrogen bonding between CEPH molecules and THY. Preliminary antimicrobial experiments via measurements of minimal inhibitory concentration (MIC) provide clear-cut evidence that the association with thymol increases the resistance of both Gram-negative and Gram-positive bacteria to the antibiotic with respect to pure CEPH as well as to physical mixtures of CEPH with thymol.

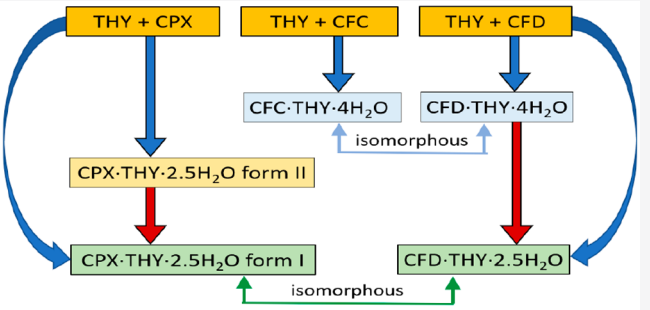

INTRODUCTION

Multicomponent molecular solids are attractive targets in the quest for novel molecular materials and are finding application in a variety of fields including pharmaceuticals,[1−6] nutraceuticals,[7−9] agrochemicals,[10−12] high-energy materials,[13−15] and pigments.[16−18] Since the solid-state packing arrangement of the building blocks (molecular and/or ionic) can dramatically affect the collective properties of the materials, it is of paramount importance to understand the relationship between the properties of the individual components and those resulting from the assembly of active ingredients and co-formers. Co-crystals have become an attractive research target, since they may provide alternative routes to new or improved properties of active molecules.[19] Pharmaceutical co-crystals composed of an active pharmaceutical ingredient (API) and a non-active ancillary co-former, selected from the Generally Recognized As Safe (GRAS) list of substances,[20] are being actively investigated by crystal engineers. It is also possible to co-crystallize an API with another API, thus forming a drug−drug (or co-drug) co-crystal.[21−27] In drug−drug co-crystals, not only the solid-state physicochemical properties of the API are altered with respect to those of the separate components, but also the pharmaceutical and biological activity may result in being significantly different because of synergistic or antagonistic effects. The first example of a co-drug was a combination of a sedative pharmaceutical pyrithyldione and a non-steroidal anti-inflammatory drug propyphenazone patented by Hoffman-La Roche in 1937.[28] In more advanced applications, APIs are chosen in a way that both have similar biological activity, and their combination as co-crystals might result in enhancement of the biological activity with respect to that of the separate components or of their physical mixture.[29−32] One of such cases has been recently reported by our research group for the co-crystals of the synthetic antibiotic ciprofloxacin with the natural antibacterial agents thymol and carvacrol (see also below).[33]

In this paper, we report our results in the co-crystallization of three representatives of the cephalosporin (CEPH) class of antibiotics, namely, cephalexin (CPX), cefradine (CFD), and cefaclor (CFC), with thymol (THY) used as a co-former (see Scheme 1).

Cephalosporins are a class of β-lactam antibiotics, extracted for the first time from the fungus *Cephalosporium acremonium*

Received: December 5, 2021
Revised: January 12, 2022

Downloaded via UNIV BOLOGNA on January 28, 2022 at 11:35:34 (UTC).
See https://pubs.acs.org/sharingguidelines for options on how to legitimately share published articles.

ACS Publications

© XXXX The Authors. Published by American Chemical Society

Scheme 1. The First Generation Cephalosporin Antibiotics Cephalexin (CPX) and Cefradine (CFD), the Second Generation Cephalosporin Cefaclor (CFC), and the Co-Former Thymol (THY) Used in Our Study[a]

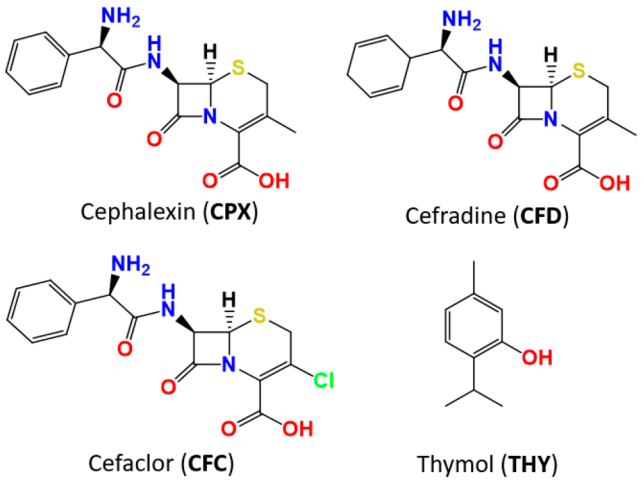

[a]CPX, CFD, and CFC were all used in their zwitterionic form.

in 1945.[34] The central nucleus of cephalosporins is formed by D-α-aminoadipic acid condensed with a β-lactam ring; this complex is called 7-aminocephalosporanic acid and represents the nucleus to which the side chains are linked for the synthesis of the various cephalosporins. The mechanism of action is carried out by synthesis inhibition of the bacterial cell wall, similarly to what was observed in the case of penicillin and derivatives.

Cephalosporins are classified into five generations according to the general characteristics of antimicrobial activity.[35] The first generation of cephalosporins, in our case cephalexin and cefradine, shows a good activity in a wide range against Gram-positive bacteria and a relatively modest activity against Gram-negative bacteria. Most of the Gram-positive cocci and oral cavity anaerobes are sensitive to the action of the first generation of cephalosporins as well as against *M. catarrhalis*, *E. coli*, *K. pneumoniae*, and *P. mirabilis*.[36] The second generation of cephalosporins is more active against Gram-negative microorganisms such as *Citrobacter* and *Enterobacter*. Cefaclor is a second-generation cephalosporin and is particularly active against *H. influenzae* and *M. catarrhalis*. In general, the second generation is more active against streptococci, *E. coli*, *P. mirabilis*, etc.[37]

Thymol [5-methyl-2-(propan-2-yl)benzenol, also known as *m*-thymol] is a natural monoterpenoid phenol derivative of *p*-cymene and is the most abundant component of the oil extracted from *Thymus vulgaris* (thyme).[38] The effective antibacterial properties of the essential oil have been investigated *in vitro* and *in vivo* against diverse Gram-negative and Gram-positive bacteria such as *S. typhimurium*, *E. coli*, and *L. monocytogenes*.[39−42] In addition to this, the herbal preparation "*Thymi aetheroleum*", listed as an "herbal medicinal product", has been assigned the GRAS (Generally Recognized As Safe) status of flavor additive[43] by FEMA (Flavor Extract Manufacturers Association).[44] The essential oils obtained from the species of the Lamiaceae family, such as the genera *Thymus*, *Ocimum*, and *Origanum* containing thymol,[45−47] have been used in the food industry since ancient times as natural preservatives in food treatment and packaging thanks to their antimicrobial, antioxidant, and anti-inflammatory properties.[48−50] Essential oils extracted from basil (*Ocimum basilicum L.*) have been traditionally used as a medicinal plant in the treatment of headaches, coughs, diarrhea, constipation, warts, worms, and kidney malfunction.[51]

As mentioned above, co-crystallization of the antibiotic ciprofloxacin (CIP hereafter) with thymol (THY) and carvacrol (CAR) yielded two families of ciprofloxacin co-crystals, one with carvacrol, namely, CIP·CAR_n (n = 2, 3, 4), and one with thymol, CIP·THY_n (n = 2, 4).[33] The effect of co-crystal formation on the antibiotic activity of ciprofloxacin was evaluated by means of standard antimicrobial tests in the cases of the co-crystals CIP·CAR_4 and CIP·THY_2, and compared with the results for the pure components and their physical mixtures: in both cases, the antimicrobial tests indicated an increase of the antimicrobial activity.

Remarkably, the outcome of analogous experiments carried out with antibiotics of the CEPH family is completely different; viz., when the co-crystals with THY are administered to Gram-negative and Gram-positive bacteria, a significant *decrease* of the antimicrobial activity, and therefore an increase of the minimal inhibitory concentration (MIC) values, is observed in comparison to the pure components and to the physical mixtures. In the following, the preparation and characterization of the co-crystals of cephalexin (CPX), cefradine (CFD), and cefaclor (CFC) with thymol (THY), namely, CPX·THY·2.5H_2O forms I and II, CFD·THY·2.5H_2O, and CFC·THY·4H_2O, respectively, will be described and the results of the antimicrobial test discussed.

EXPERIMENTAL SECTION

CPX and CFD used in this work were purchased from Tokyo Chemical Industry (TCI); CFC, THY, and all solvents were purchased from Sigma-Aldrich. All reagents and solvents were used without further purification.

Solution Synthesis. *Synthesis of CFD·THY·2.5H_2O and CFC·THY·4H_2O.* In separate experiments, CFD (25 mg, 0.071 mmol) and CFC (25 mg, 0.068 mmol) were solubilized in 2 mL of water; sonication was used to accelerate the dissolution process. As thymol is insoluble in water, a solution of THY (15.9 mg, 0.106 mmol for CFD; 15.3 mg, 0.102 mmol for CFC) was prepared in 1 mL of EtOH, which was then added to both CFD and CFC aqueous solutions. The vials containing the mixture were covered with Parafilm and stored at 5 °C. A similar approach was used by Kemperman et al. in the preparation of clathrate-type complexes of cephalosporins.[59−61] Single crystals suitable for X-ray diffraction were collected after 2 days from the crystallization batches.

Synthesis of CPX·THY·2.5H_2O Forms I and II. CPX (25 mg, 0.072 mmol) was solubilized in 2 mL of water; sonication was used to accelerate the dissolution process. A solution obtained by dissolving THY (16.2 mg, 0.108 mmol) in 1 mL of EtOH/CH_2Cl_2 50:50 was then added to the CPX aqueous solution. The vial containing the resulting mixture was partially covered with Parafilm and stored under a fume hood at room temperature. After 2 days, single crystals of form II were recovered, while, after 2 more days, only crystals of form I were found in the same crystallization batch.

Synthesis by Slurry. In three separate experiments, CPX (100 mg, 0.288 mmol), CFD (100 mg, 0.286 mmol), and CFC (100 mg, 0.272 mmol) were slurried with THY in a 1:1 stoichiometric ratio (43.3, 42.9, and 40.9 mg, respectively) for 48 h in 2 mL of water and 3 drops (150 μL) of EtOH. After filtration, the solid material was left to dry out under ambient conditions.

Mechanochemical Synthesis. In three separate experiments, CPX (50 mg, 0.144 mmol), CFD (50 mg, 0.143 mmol), and CFC (50 mg, 0.136 mmol) were milled with thymol in a 1:1 stoichiometric ratio (21.6, 21.5, and 20.4 mg, respectively) in a RETSCH MM200

https://doi.org/10.1021/acs.cgd.1c01435
Cryst. Growth Des. XXXX, XXX, XXX−XXX

(mixer mill) for 1 h (30 min + 30 min with a 5 min break) at 20 Hz milling frequency, using a 5 mL agate jar with three agate balls of 5 mm diameter; 2 drops of water (100 μL) were added to the solid mixture (liquid-assisted grinding, LAG). The product was left to dry out at room temperature and directly collected from the jar.

Crystallization. Single crystals of CFC·THY·4H_2O and of CPX·THY·2.5H_2O were crystallized from a mixture of three solvents, namely, ethanol, dichloromethane, and water. CPX·THY·2.5H_2O was obtained in two polymorphic forms; as form II is metastable, all solubility and antimicrobial activity measurements were carried out on form I (see below). In the case of CFD·THY·2.5H_2O, the structure was found to be isomorphous with that of CPX·THY·2.5H_2O form I. Single crystals of CPX·THY·4H_2O and of CFC·THY·2.5H_2O could not be obtained even by attempting heteroseeding crystallization with preformed crystals of isomorphous CFC·THY·4H_2O or CPX·THY·2.5H_2O form I. In the former case, the addition of the seeds of CFC·THY·4H_2O led to the immediate crystallization of a polycrystalline powder that was characterized as CPX·THY·2.5H_2O form I. Analogously, the addition of the seeds of CPX·THY·2.5H_2O form II to the solution of CFC and THY did not affect the crystallization, and CFC·THY·4H_2O was obtained.

Powder X-ray Diffraction. Room temperature powder X-ray diffraction patterns were collected on a PANalytical X'Pert Pro automated diffractometer equipped with an X'Celerator detector in Bragg–Brentano geometry, using Cu Kα radiation (λ = 1.5418 Å) without a monochromator in the 3–40° 2θ range (step size 0.033°; time/step 20 s; Soller slit 0.04 rad; anti-scatter slit $^1/_2$; divergence slit $^1/_4$; 40 mA × 40 kV).

Single Crystal X-ray Diffraction. Single crystal X-ray diffraction data were collected at RT for CFC·THY·4H_2O, CPX·THY·2.5H_2O form I, and at 100 K for CPX·THY·2.5H_2O form II, with an Oxford Diffraction X'Calibur instrument equipped with a graphite monochromator and a CCD detector. Unit cell parameters for all compounds discussed herein are reported in Table SI-1. The structures were solved by the intrinsic phasing methods and refined by least-squares methods against F^2 using SHELXT-2016[55] and SHELXL-2018[56] with the Olex^2 interface.[57] Non-hydrogen atoms were refined anisotropically. Hydrogen atoms were added in calculated positions. The software Mercury 4.1.2[58] was used to analyze and represent the crystal packing.

Testing of Antimicrobial Activity. Antimicrobial activity was tested by the broth microdilution method, according to the guidelines of the two established organizations and committees on antimicrobial susceptibility testing, the CLSI and EUCAST.[52,53] For comparison, tests were conducted on suspensions of thymol, CEPH, physical mixtures, and co-crystals in 10 progressive concentrations ranging from 512 to 1 μg/mL. All suspensions were tested in parallel, using as reference strains different types of bacteria pretested with different standard methods (automatic and semiautomatic) to determine their MICs.[54] Both sensitive and resistant strains, with a MIC that fell within the concentration range of 1 to 512 μg/mL, were considered.

Drug and co-crystal solutions/suspensions were prepared in the same way for all samples, namely, 30.720 mg of analyte in 15 mL of physiological solution of sodium chloride 0.45% (e.g., 30.720 mg of CEPH in 15 mL of physiological solution or 30.720 mg of co-crystal in 15 mL of physiological solution). Physical mixtures were prepared in stoichiometric ratios via simple mixing of drug dispersions and essential oil dispersions.

The antibacterial assay was carried out for all samples by using a 96-well microtiter plate; wells were filled with 50 μL of cation adjusted MH broth from well 2 to well 12; then, 100 μL of sample solution/dispersion were added and put in well 1. After that, the serial dilutions were obtained by taking 50 μL of MH broth from well 1 to well 2 and then proceeding in the same way from well 2 to well 3, etc., until well 11. This procedure resulted in 1:2 serial dilutions ranging from 512 to 1 μg/mL from well 2 to well 11. In this way, well 1 was the negative control to verify that the sample was not contaminated, while well 12 was the positive control to check for bacterial growth and was used as a comparison to evaluate the MIC well. Table SI-2 reports the results of all antimicrobial tests by comparing MIC (μg/mL) in the cases of CEPH, of CEPH and THY as a physical mixture, and of the co-crystals for a series of both susceptible and resistant strains. The percentage molar differences in CEPH between the MIC of each CEPH and the MIC of the corresponding co-crystals are also reported (column 4).

Solubility Measurements. Solubility in water of (i) CPX (11.3 mg), CFD (10 mg), and CFC (5 mg); (ii) thymol (10 mg); and (iii) the co-crystals CFD·THY·2.5H_2O (10 mg), CPX·THY·2.5H_2O form I (9.8 mg), and CFC·THY·4H_2O (10 mg) was measured three times at room temperature by a stepwise procedure: each single material was suspended in 1 mL of water (quantities in mg are indicated above) in a 20 mL glass vial, and the volume of water was increased by 0.5 mL at a time; sonication (30 s^{-1} min, 95 W, 50/60 Hz) was applied after each addition. Determination of complete dissolution was based entirely on visual observation. Results are reported in Table 1.

Table 1. Solubility in Water of the Compounds Discussed Herein

compound	solubility[a] (mg/mL)	solubility (mol/L)
THY	insoluble	insoluble
CFD	6.6(3)	1.8×10^{-2}
CPX	5.6(2)	1.5×10^{-2}
CFC	5.1(2)	1.4×10^{-2}
CFD·THY·2.5H_2O	1.1(3)	2.1×10^{-3}
CPX·THY·2.5H_2O	1.4(4)	2.6×10^{-3}
CFC·THY·4H_2O	1.4(3)	2.4×10^{-3}

[a]Values in parentheses are standard deviations over three measurements.

RESULTS AND DISCUSSION

Co-crystallization of the three cephalosporins with thymol invariably resulted in the formation of hydrated co-crystals. As discussed in the Experimental Section, the reaction between cephalosporins and thymol was conducted under three different conditions, i.e., solution, slurry, and liquid-assisted grinding (LAG). The relationship between the co-crystallization processes and the products obtained is depicted in Scheme 2.

Co-Crystallization of Cefaclor with Thymol. Co-crystallization of CFC with THY invariably resulted in the

Scheme 2. Co-Crystallization Results of Thymol (THY) with Cephalexin (CPX), Cefaclor (CFC), and Cefradine (CFD)[a]

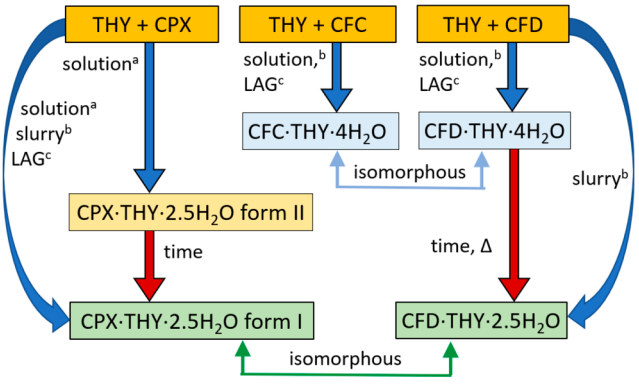

[a]Solvents used are (a) H_2O–EtOH–CH_2Cl_2, (b) H_2O–EtOH, and (c) H_2O.

https://doi.org/10.1021/acs.cgd.1c01435
Cryst. Growth Des. XXXX, XXX, XXX–XXX

formation of CFC·THY·4H_2O, irrespective of the process employed (see Scheme 2). Crystalline CFC·THY·4H_2O is composed of distinct layers of CFC and thymol molecules (Figure 1a). Water molecules are interposed in the layers of zwitterionic CFC molecules, interacting with them via hydrogen bonds. CFC molecules interact with each other via $NH_3^+\cdots O_{COO^-}$ hydrogen bonds (Figure 1b), while they do not form hydrogen bonds with the hydroxyl groups of the thymol molecules (Figure 1c).

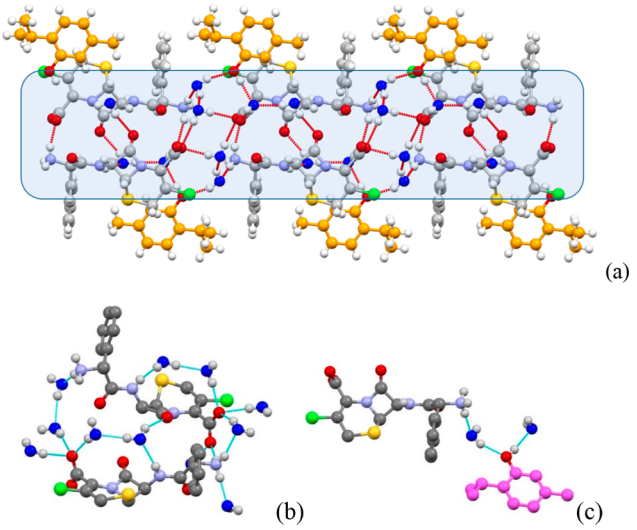

Figure 1. Crystal packing of cefaclor and thymol molecules in crystalline CFC·THY·4H_2O. (a) Projections in the *bc*-plane of packing portions for crystalline CFC·THY·4H_2O evidencing the "segregation" of the hydrophilic region (light-blue rectangle) in the structure (O_W atoms in blue). (b) Hydrogen bonding interactions between CFC and water molecules and (c) between CFC, water, and THY (C_{THY} in pink; H atoms omitted for clarity).

Co-Crystals of Cephalexin with Thymol. The co-crystallization of CPX with THY via ball milling with a few drops of water or via slurry in H_2O/EtOH solution results in the formation of CPX·THY·2.5H_2O. Single crystals for X-ray structural determination could only be grown with a double-layer approach at the interface of a solution of CPX in water and a solution of thymol in EtOH:CH_2Cl_2. Other choices of solvents or the use of mixtures of two solvents only yielded polycrystalline CPX·THY·2.5H_2O. Together with single crystals of the desired form, however, the concomitant formation of a few crystals of a polymorphic form was detected, i.e., CPX·THY·2.5H_2O form II; in a matter of days, though, all crystals of form II had converted, in the presence of residual solution, into stable form I. While crystals of form I are stable under X-rays and data could be collected under ambient conditions, data for crystalline CPX·THY·2.5H_2O form II had to be collected at 100 K. Crystalline CPX·THY·2.5H_2O form II could not be detected in any other solid-state or solution experiment.

Crystalline CPX·THY·2.5H_2O form I is shown in Figure 2. The crystal packing resembles the one observed for CFC·THY·4H_2O. Once again, distinct layers of thymol and of CPX molecules are present (Figure 2a). Water molecules are interposed within the layers of CPX molecules acting as a hydrogen bonding bridge between CPX and THY molecules. O_{H_2O} acts as a hydrogen bonding acceptor for H_{OH} of THY molecules, and both H_{H_2O}, in turn, interact via $OH\cdots O_{COO^-}$ hydrogen bonding with two different molecules of CPX (Figure 2b). CPX molecules interact via $NH_3^+\cdots O_{COO^-}$ hydrogen bonds with each other (Figure 2b). The protonated amino groups of one CPX molecule interact via hydrogen bonding with the carboxylate groups of two other CPX molecules.

Segregation of the hydrophobic and hydrophilic regions is a feature also shared by crystalline CPX·THY·2.5H_2O form II, as is shown in Figure 3a. Figure 3b shows the absence of direct hydrogen bonding interactions between thymol and cephalexin molecules, connected one to the other via bridging water molecules.

Form I and form II of CPX·THY·2.5H_2O differ mainly because of the conformation due to the torsion of the carboxylate groups; see Figure 4 for a comparison.

Co-Crystals of Cefradine with Thymol. The co-crystallization of cefradine with thymol showed some similarities with both cefaclor and cephalexin (see Scheme 2). Liquid-assisted grinding resulted in the formation of the co-crystal CFD·THY·4H_2O, isomorphous with CFC·THY·4H_2O, as evidenced by a comparison of the measured XRPD pattern of CFD·THY·4H_2O with that calculated on the basis of single crystal data for CFC·THY·4H_2O (see Figure 5).

Single crystals of CFD·THY·4H_2O were grown in a similar way as the ones for the cefaclor co-crystal. However, these crystals were much less stable, rapidly degrading during data collection, even if the temperature was lowered to 100 K. Consequently, the crystals were left under ambient conditions for 12 h, and afterward, an XRPD pattern was collected. As it can be appreciated from Figure 6, a phase change had taken

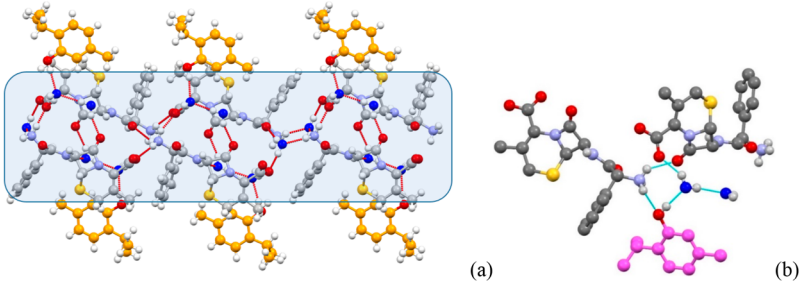

Figure 2. Crystal packing of cephalexin and thymol molecules in crystalline CPX·THY·2.5H_2O form I. (a) Projection of a packing portion of crystalline CPX·THY·2.5H_2O form I, evidencing the layer of THY molecules hydrogen bonded to CPX and water molecules (O_W in blue). (b) Hydrogen bonding interactions between CPX, water, and THY molecule (C_{THY} in pink; H atoms omitted for clarity).

https://doi.org/10.1021/acs.cgd.1c01435
Cryst. Growth Des. XXXX, XXX, XXX−XXX

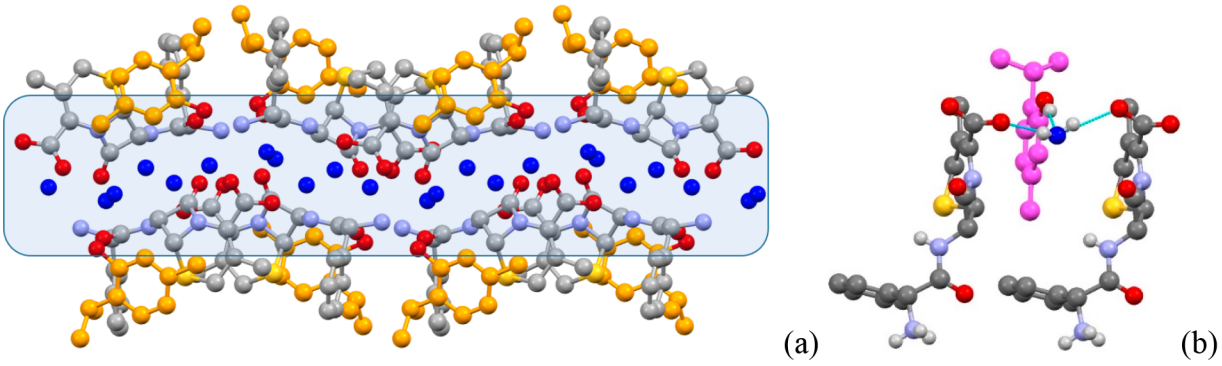

Figure 3. Segregation of the hydrophilic regions in crystalline CPX·THY·2.5H_2O form II (a) (H atoms and H-bonds not shown for clarity); hydrogen bonding interactions between CPX, water, and THY molecules (b); hydrogen bonding interactions mediated by a water molecule between CPX molecules (c) (carbon atoms of THY in pink, O_W in blue; hydrogens omitted for clarity).

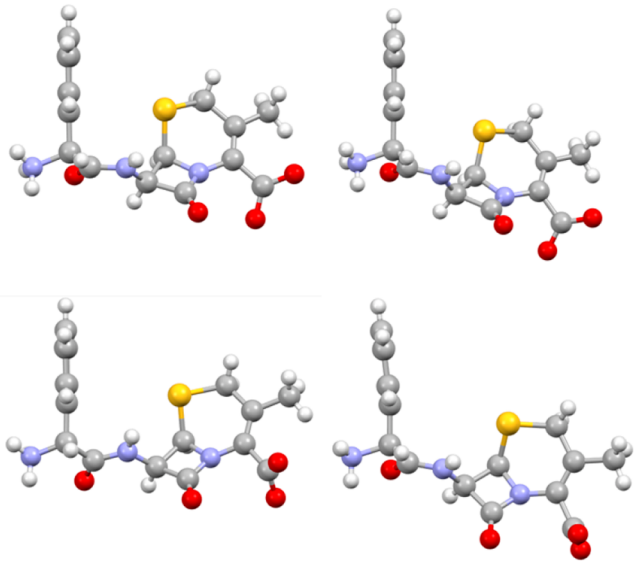

Figure 4. Conformation of the CPX molecules in form II (top) and form I (bottom): the main difference between the two forms is in the torsion of the carboxylate groups.

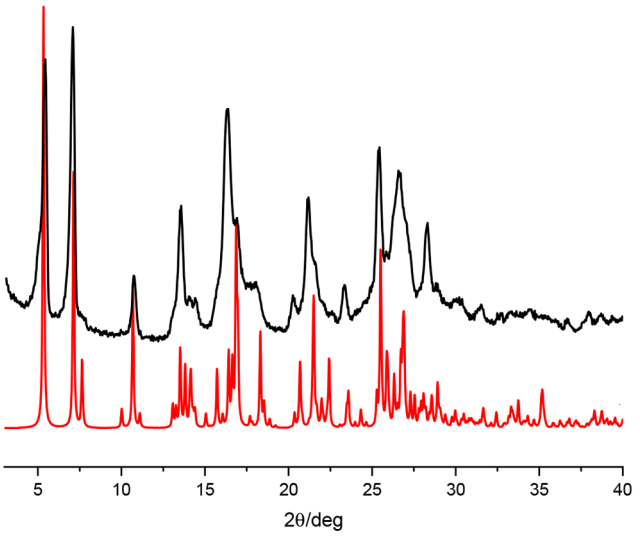

Figure 5. Comparison between the experimental powder X-ray pattern for CFD·THY·4H_2O (black line, top) and the one calculated on the basis of single crystal data for CFC·THY·4H_2O (red line, bottom).

place. This last phase was later prepared again (i) via slurry of CFD·THY·4H_2O and also (ii) directly from crystalline CFD·THY·4H_2O as obtained from the LAG process and stored under ambient conditions in a closed vial for 48 h. On the basis of the comparison of the X-ray patterns, this second form seems to be isomorphous with the stable form of CPX·THY·2.5H_2O, i.e., form I (see Figure 6).

Antimicrobial Activity. The results of the antimicrobial activity testing are now discussed. As described in the Experimental Section, the same strains were tested for each system. Results referring to the strains that provided growth inhibition values considered of interest for the purposes of the work are discussed. Table SI-2 lists the minimal inhibitory concentration (MIC) values for all CEPH, for CEPH and THY physical mixtures, and for the CEPH·THY·$n$$H_2O$ co-crystals, together with the percentage concentration increase, calculated after normalization of the data, necessary for mixed systems to show the same antimicrobial effect as pure CEPH compounds. As can be seen from the examples listed in Table 2, all co-crystals were found to give growth inhibition at concentrations invariably higher than CEPH alone. In the cases where a specific strain was found highly susceptible to the antibacterial, the corresponding co-crystals were not tested. However, when these quantities are normalized on the basis of the co-crystal formulas, differences begin to appear. Growth inhibition with CFD·THY·2.5H_2O requires a larger dose of cephalosporin compared to the other co-crystals described in this work. CFC·THY·4H_2O is considerably more efficient, as the increase of the antibiotic dose necessary to reach the MIC value is lower than that for the other systems considered. An analogous behavior could also be observed for the physical mixtures of CEPH and THY, although they present, on average, similar or slightly lower growth inhibition concentrations, based on normalized data, with respect to co-crystals. Finally, pure THY shows growth inhibition at very high values (not reported in Table 2), which are on the mg/mL scale, therefore not comparable to those for CEPH and co-crystals.

CONCLUSIONS

Co-crystallization of CEPH molecules with thymol was successful in yielding a class of closely related hydrated co-crystals with a 1:1 stoichiometry between the CEPH molecules

https://doi.org/10.1021/acs.cgd.1c01435
Cryst. Growth Des. XXXX, XXX, XXX−XXX

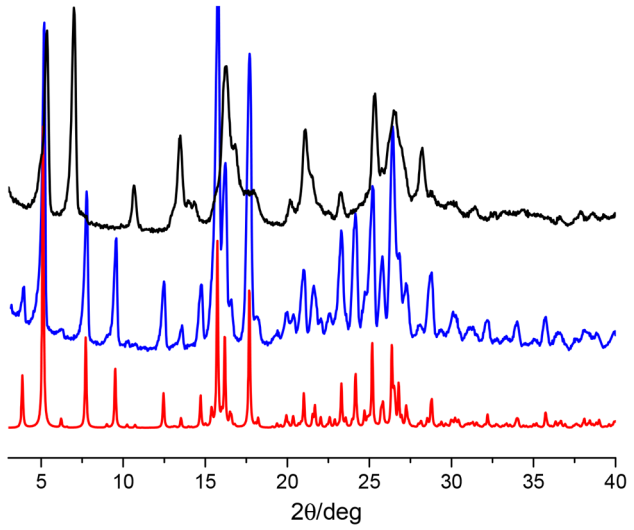

Figure 6. Comparison between the experimental XRPD patterns for CFD·THY·4H_2O as obtained from LAG (black line, top), the pattern obtained after 12 h under ambient conditions (blue line, middle), and the pattern calculated on the basis of single crystal data for CPX·THY·2.5H_2O form I (red line, bottom). As blue and red lines are superimposable, it can be inferred that a complete transformation has taken place from CFD·THY·4H_2O to a co-crystal isomorphous with CPX·THY·2.5H_2O form I, i.e., CFD·THY·2.5H_2O.

and THY. In all cases (with the exception of the low temperature form of CPX·THY·2.5H_2O), THY is not linked directly to the CEPH molecules but is linked to the antibiotic via water bridges. It is perhaps worth mentioning that all crystal structures of CPX, CFD, and CFC, currently available in the CSD database,[62] are hydrates, confirming the strong affinity of the CEPH molecules with water.

The antimicrobial activity of the co-crystals CPX·THY·2.5H_2O form II, CFD·THY·2.5H_2O, and CFC·THY·4H_2O was compared with that of CEPH alone, as well as with that of physical mixtures of CEPH with THY in adequate stoichiometric ratios, against a reference strain of different bacteria both susceptible and not susceptible to CEPH. THY was also tested. At variance with what was previously observed in the cases of the co-crystals of ciprofloxacin with thymol,[33] the CEPH co-crystallization products show exactly the opposite behavior in terms of antimicrobial activity. The co-crystals CPX·THY·2.5H_2O form II, CFD·THY·2.5H_2O, and CFC·THY·4H_2O are less effective against the bacteria than the pure active ingredient.

This apparently negative result is extremely interesting and prompts the investigation of the reasons for such a different behavior. Clearly, the two classes of antibiotics have very different biological activity (interaction with different active sites on the proteins, etc.), and the comparison cannot be between the two classes of compounds. Rather, the focus of this crystal engineering paper is on the observation that the same conceptual approach, namely, the construction of aggregates between natural antibiotics such as thymol and carvacrol and the APIs, may also cause an inhibition of the activity. This should also raise a warning, as it cannot be excluded a priori that approved substances commonly used for human consumption, as is the case of thymol, might have an impact on the pharmacological effects of antibiotics. More explorative work should be conducted with this caveat in mind.

It may also be worth noting that the solubilities in water of the co-crystals are an order of magnitude less than those of the pure CEPH (see Table 1); while the molar solubility of the CEPH molecules, when associated to THY, is significantly lower than the solubility of the free cephalosporines, THY

Table 2. Percentual Increase in Minimal Inhibition Concentration (MIC) Normalized on the Amount of CEPH (mM) for the Co-Crystals CFD·THY·2.5H_2O, CPX·THY·2.5H_2O, and CFC·THY·4H_2O with Respect to the Pure Cephalosporins CFD, CPX, and CFC, Respectively

	CFD·THY·2.5H_2O vs CFD	CPX·THY·2.5H_2O vs CPX	CFC·THY·4H_2O vs CFC
	Gram-Positive Bacteria		
Enterococcus faecalis	926	28	148
Staphylococcus aureus MRSA	926	28	148
Staphylococcus epidermidis	413	156	148
	Gram-Negative Bacteria		
Alcaligenes faecalis	413	[a]	398
Citrobacter freundii	[a]	156	[a]
Citrobacter koseri	[a]	[a]	24
Enterobacter cloacae	413	156	[a]
Enterobacter aerogenes	≥4004[c]	[a]	[a]
Escherichia coli	[a]	156	24
Escherichia coli ESβL+[b]	≥413[c]	924	148
Salmonella cholaeresuis	1952	156	148
Hafnia alvei	28	≥8093[c]	148
Klebsiella oxytoca	[a]	28	[a]
Morganella morganii	4004	8093	[a]
Proteus mirabilis ESβL+[b]	8109	1948	≥1948[c]
Proteus mirabilis	4004	3996	≥3996[c]
Providencia stuartii	1952	[a]	[a]

[a]Notes: co-crystal was not tested because the corresponding CEPH gives MIC values below the measurement limit for the specific antibacterial-susceptible strain. [b]ESβL+ stands for extended spectrum beta-lactamase. [c]The symbol ≥ is used to indicate that higher concentrations have not been investigated; therefore, the real MIC value could not be ascertained.

https://doi.org/10.1021/acs.cgd.1c01435
Cryst. Growth Des. XXXX, XXX, XXX−XXX

shows exactly the opposite phenomenon, becoming soluble in water.

In summary, the evaluation of the MIC values in the cases discussed herein is consistent with an inhibition effect by THY on the antibiotic activity of the three CEPH molecules upon formation of co-crystals with THY. The inhibition is less pronounced with the new generation cephalosporines. However, whether this inhibition is due to a different permeability[63] of the CEPH co-crystals or, more simply, to the difference in solubility of the co-crystals with respect to the CEPH on their own needs to be investigated further with *ad hoc* studies *in vivo* also by considering the opposite behavior shown by the co-crystals of ciprofloxacin with thymol, which appears to be more soluble by a factor of 2 with respect to the antibiotic.[33] Work in this direction is in progress and will be the subject of future reports.

■ ASSOCIATED CONTENT

Supporting Information

The Supporting Information is available free of charge at https://pubs.acs.org/doi/10.1021/acs.cgd.1c01435.

Single crystal and powder X-ray diffraction and antimicrobial tests (PDF)

Accession Codes

CCDC 2125511−2125513 contain the supplementary crystallographic data for this paper. These data can be obtained free of charge via www.ccdc.cam.ac.uk/data_request/cif, or by emailing data_request@ccdc.cam.ac.uk, or by contacting The Cambridge Crystallographic Data Centre, 12 Union Road, Cambridge CB2 1EZ, UK; fax: +44 1223 336033.

■ AUTHOR INFORMATION

Corresponding Authors

Vittorio Sambri − *U.O. Microbiologia - Laboratorio Unico Centro Servizi AUSL Romagna, 47522 Pievesestina di Cesena, FC, Italy; Dipartimento di Medicina Specialistica, Diagnostica e Sperimentale Università di Bologna, 40138 Bologna, Italy*; Email: vittorio.sambri@unibo.it

Dario Braga − *Dipartimento di Chimica "Giacomo Ciamician", Università di Bologna, 40126 Bologna, Italy*; orcid.org/0000-0003-4162-4779; Email: dario.braga@unibo.it

Authors

Cecilia Fiore − *Dipartimento di Chimica "Giacomo Ciamician", Università di Bologna, 40126 Bologna, Italy*

Alessandra Baraghini − *Dipartimento di Farmacia e Biotecnologie "FABIT", Università di Bologna, 40126 Bologna, Italy*

Oleksii Shemchuk − *Institute of Condensed Matter and Nanosciences, UCLouvain, B-1348 Louvain-la-Neuve, Belgium*; orcid.org/0000-0003-3003-3922

Manuela Morotti − *U.O. Microbiologia - Laboratorio Unico Centro Servizi AUSL Romagna, 47522 Pievesestina di Cesena, FC, Italy*

Fabrizia Grepioni − *Dipartimento di Chimica "Giacomo Ciamician", Università di Bologna, 40126 Bologna, Italy*; orcid.org/0000-0003-3895-0979

Complete contact information is available at: https://pubs.acs.org/10.1021/acs.cgd.1c01435

Author Contributions

The manuscript was written through contributions of all authors. All authors have given approval to the final version of the manuscript.

Notes

The authors declare no competing financial interest.

■ ACKNOWLEDGMENTS

Financial support from the University of Bologna is acknowledged.

■ REFERENCES

(1) Stanton, M. K.; Bak, A. Physicochemical properties of pharmaceutical co-crystals: A case study of ten AMG 517 co-crystals. *Cryst. Growth Des.* **2008**, *8* (10), 3856−3862.

(2) Wouters, J.; Quéré, L. *Pharmaceutical salts and co-crystals*; Royal Society of Chemistry: 2011.

(3) Steed, J. W. The role of co-crystals in pharmaceutical design. *Trends Pharmacol. Sci.* **2013**, *34* (3), 185−93.

(4) Golob, S.; Perry, M.; Lusi, M.; Chierotti, M. R.; Grabnar, I.; Lassiani, L.; Voinovich, D.; Zaworotko, M. J. Improving Biopharmaceutical Properties of Vinpocetine Through Cocrystallization. *J. Pharm. Sci.* **2016**, *105* (12), 3626−3633.

(5) Guo, C.; Zhang, Q.; Zhu, B.; Zhang, Z.; Bao, J.; Ding, Q.; Ren, G.; Mei, X. Pharmaceutical Cocrystals of Nicorandil with Enhanced Chemical Stability and Sustained Release. *Cryst. Growth Des.* **2020**, *20* (10), 6995−7005.

(6) Alvarez-Lorenzo, C.; Castiñeiras, A.; Frontera, A.; García-Santos, I.; González-Pérez, J. M.; Niclós-Gutiérrez, J.; Rodríguez-González, I.; Vílchez-Rodríguez, E.; Zarřba, J. K. Recurrent motifs in pharmaceutical cocrystals involving glycolic acid: X-ray characterization, Hirshfeld surface analysis and DFT calculations. *CrystEngComm* **2020**, *22* (40), 6674−6689.

(7) Bethune, S. J.; Schultheiss, N.; Henck, J. O. Improving the Poor Aqueous Solubility of Nutraceutical Compound Pterostilbene through Cocrystal Formation. *Cryst. Growth Des.* **2011**, *11* (7), 2817−2823.

(8) Bevill, M. J.; Vlahova, P. I.; Smit, J. P. Polymorphic Cocrystals of Nutraceutical Compound p-Coumaric Acid with Nicotinamide: Characterization, Relative Solid-State Stability, and Conversion to Alternate Stoichiometries. *Cryst. Growth Des.* **2014**, *14* (3), 1438−1448.

(9) Barbas, R.; Bofill, L.; de Sande, D.; Font-Bardia, M.; Prohens, R. Crystal engineering of nutraceutical phytosterols: new cocrystal solid solutions. *CrystEngComm* **2020**, *22* (25), 4210−4214.

(10) Nauha, E.; Nissinen, M. Co-crystals of an agrochemical active - A pyridine-amine synthon for a thioamide group. *J. Mol. Struct.* **2011**, *1006* (1−3), 566−569.

(11) Powell, K. A.; Croker, D. M.; Rielly, C. D.; Nagy, Z. K. PAT-based design of agrochemical co-crystallization processes: A case-study for the selective crystallization of 1:1 and 3:2 co-crystals of p-toluenesulfonamide/triphenylphosphine oxide. *Chem. Eng. Sci.* **2016**, *152*, 95−108.

(12) Julien, P. A.; Germann, L. S.; Titi, H. M.; Etter, M.; Dinnebier, R. E.; Sharma, L.; Baltrusaitis, J.; Friscic, T. In situ monitoring of mechanochemical synthesis of calcium urea phosphate fertilizer cocrystal reveals highly effective water-based autocatalysis. *Chemical Science* **2020**, *11* (9), 2350−2355.

(13) Kent, R. V.; Wiscons, R. A.; Sharon, P.; Grinstein, D.; Frimer, A. A.; Matzger, A. J. Cocrystal Engineering of a High Nitrogen Energetic Material. *Cryst. Growth Des.* **2018**, *18* (1), 219−224.

(14) Gamekkanda, J. C.; Sinha, A. S.; Aakeroy, C. B. Cocrystals and Salts of Tetrazole-Based Energetic Materials. *Cryst. Growth Des.* **2020**, *20* (4), 2432−2439.

(15) Tan, Y.; Liu, Y.; Wang, H.; Li, H.; Nie, F.; Yang, Z. Different Stoichiometric Ratios Realized in Energetic-Energetic Cocrystals Based on CL-20 and 4,5-MDNI: A Smart Strategy to Tune Performance. *Cryst. Growth Des.* **2020**, *20* (6), 3826−3833.

(16) Bucar, D. K.; Filip, S.; Arhangelskis, M.; Lloyd, G. O.; Jones, W. Advantages of mechanochemical cocrystallisation in the solid-state chemistry of pigments: colour-tuned fluorescein cocrystals. *CrystEngComm* **2013**, *15* (32), 6289−6291.
(17) Li, M. Q.; Zhang, Z.; Zhang, Q.; Peng, B.; Zhu, B.; Wang, J. R.; Liu, L. Y.; Mei, X. F. Fine-Tuning the Colors of Natural Pigment Emodin with Superior Stability through Cocrystal Engineering. *Cryst. Growth Des.* **2018**, *18* (10), 6123−6132.
(18) Karangutkar, A. V.; Ananthanarayan, L. Co-crystallization of Basella rubra extract with sucrose: Characterization of co-crystals and evaluating the storage stability of betacyanin pigments. *Journal of Food Engineering* **2020**, *271*, 109776.
(19) Guo, M.; Sun, X.; Chen, J.; Cai, T. Pharmaceutical cocrystals: A review of preparations, physicochemical properties and applications. *Acta Pharmaceutica Sinica B* **2021**, *11* (8), 2537−2564.
(20) http://www.fda.gov/Food/IngredientsPackagingLabeling/GRAS/.
(21) Thipparaboina, R.; Kumar, D.; Chavan, R. B.; Shastri, N. R. Multidrug co-crystals: towards the development of effective therapeutic hybrids. *Drug Discov Today* **2016**, *21* (3), 481−90.
(22) Kavanagh, O. N.; Albadarin, A. B.; Croker, D. M.; Healy, A. M.; Walker, G. M. Maximising success in multidrug formulation development: A review. *J. Controlled Release* **2018**, *283*, 1−19.
(23) Thakuria, R.; Sarma, B. Drug-Drug and Drug-Nutraceutical Cocrystal/Salt as Alternative Medicine for Combination Therapy: A Crystal Engineering Approach. *Crystals* **2018**, *8* (2), 101.
(24) Kaur, R.; Cavanagh, K. L.; Rodriguez-Hornedo, N.; Matzger, A. J. Multidrug Cocrystal of Anticonvulsants: Influence of Strong Intermolecular Interactions on Physiochemical Properties. *Cryst. Growth Des* **2017**, *17* (10), 5012−5016.
(25) Drozd, K. V.; Manin, A. N.; Churakov, A. V.; Perlovich, G. L. Novel drug-drug cocrystals of carbamazepine with para-aminosalicylic acid: screening, crystal structures and comparative study of carbamazepine cocrystal formation thermodynamics. *CrystEngComm* **2017**, *19* (30), 4273−4286.
(26) Liu, F.; Song, Y.; Liu, Y. N.; Li, Y. T.; Wu, Z. Y.; Yan, C. W. Drug-Bridge-Drug Ternary Cocrystallization Strategy for Antituberculosis Drugs Combination. *Cryst. Growth Des.* **2018**, *18* (3), 1283−1286.
(27) Bordignon, S.; Cerreia Vioglio, P.; Priola, E.; Voinovich, D.; Gobetto, R.; Nishiyama, Y.; Chierotti, M. R. Engineering Codrug Solid Forms: Mechanochemical Synthesis of an Indomethacin-Caffeine System. *Cryst. Growth Des.* **2017**, *17* (11), 5744−5752.
(28) Roche, F. H. Artificial Pneumothorax on Statistical Trial. *Lancet* **1937**, *229*, 597.
(29) Nugrahani, I.; Asyarie, S.; Soewandhi, S. N.; Ibrahim, S. The Antibiotic Potency of Amoxicillin-Clavulanate Co-Crystal. *International Journal of Pharmacology* **2007**, *3* (6), 475−481.
(30) Bhatt, P. M.; Azim, Y.; Thakur, T. S.; Desiraju, G. R. Co-Crystals of the Anti-HIV Drugs Lamivudine and Zidovudine. *Cryst. Growth Des.* **2009**, *9* (2), 951−957.
(31) Almansa, C.; Mercè, R.; Tesson, N.; Farran, J.; Tomàs, J.; Plata-Salamán, C. R. Co-crystal of Tramadol Hydrochloride-Celecoxib (ctc): A Novel API-API Co-crystal for the Treatment of Pain. *Cryst. Growth Des.* **2017**, *17* (4), 1884−1892.
(32) Shemchuk, O.; Braga, D.; Grepioni, F.; Turner, R. J. Co-crystallization of antibacterials with inorganic salts: paving the way to activity enhancement. *Rsc Advances* **2020**, *10* (4), 2146−2149.
(33) Shemchuk, O.; d'Agostino, S.; Fiore, C.; Sambri, V.; Zannoli, S.; Grepioni, F.; Braga, D. Natural Antimicrobials Meet a Synthetic Antibiotic: Carvacrol/Thymol and Ciprofloxacin Cocrystals as a Promising Solid-State Route to Activity Enhancement. *Cryst. Growth Des.* **2020**, *20* (10), 6796−6803.
(34) Nath, A. P.; Balasubramanian, A.; Ramalingam, K. Cephalosporins: An imperative antibiotic over the generations. *Int. J. Res. Pharm. Sci.* **2020**, *11*, 623−629.
(35) Rossi, F.; Cuomo, V.; Riccardi, C. *Farmacologia, Principi di base e applicazioni terapeutiche*, 3rd ed.; Edizioni Minerva Medica: 2017; pp 698−701.
(36) Beers, M. H.; Fletcher, A. J.; Jones, T. V.; Porter, R.; Berkwitz, M.; Kaplan, J. L. *The Merck manual of medical information*, 2nd home ed.; Merck Research Laboratories: Whitehouse Station, NJ, 2003.
(37) Brunton, L.; Blumenthal, D.; Buxton, I.; Parker, K. *Goodman and Gilman's Manual of Pharmacology and Therapeutics*, 1st ed.; McGraw-Hill Professional: 2007.
(38) Marino, M.; Bersani, C.; Comi, G. Antimicrobial activity of the essential oils of Thymus vulgaris L. measured using a bioimpedometric method. *Journal of Food Protection* **1999**, *62*, 1017−1023.
(39) Altieri, C.; Speranza, B.; Del Nobile, M. A.; Sinigaglia, M. Suitability of bifidobacteria and thymol as biopreservatives in extending the shelf life of fresh packed plaice fillets. *J. Appl. Microbiol.* **2005**, *99*, 1294−1302.
(40) Valero, D.; Valverde, J. M.; Martínez-Romero, D.; Guillén, F.; Castillo, S.; Serrano, M. The combination of modified atmosphere packaging with eugenol or thymol to maintain quality, safety and functional properties of table grapes. *Postharvest Biology and Technology* **2006**, *41*, 317−327.
(41) Falcone, P.; Speranza, B.; Del Nobile, M. A.; Corbo, M. R.; Sinigaglia, M. A study on the antimicrobial activity of thymol intended as a natural preservative. *Journal of Food Protection* **2005**, *68* (8), 1664−1670.
(42) Zhou, F.; Ji, B.; Zhang, H.; Jiang, H.; Yang, Z.; Li, J.; Li, J.; Yan, W. The antibacterial effect of cinnamaldehyde, thymol, carvacrol and their combinations against the foodborne pathogen salmonella typhimurium. *Journal of Food Safety* **2007**, *27*, 124−133.
(43) Ash, M.; Ash, I. *Handbook of preservatives*; Synapse Information Resources, Inc.: 2004.
(44) https://www.femaflavor.org/flavor-library/thymol.
(45) Sarwar, A.; Latif, Z. GC-MS characterisation and antibacterial activity evaluation of Nigella sativa oil against diverse strains of Salmonella. *Natural Product Research* **2015**, *29* (5), 447−451.
(46) Licata, M.; Tuttolomondo, T.; Dugo, G.; Ruberto, G.; Leto, C.; Napoli, E. M.; Rando, R.; Rita Fede, M.; Virga, G.; Leone, R.; La Bella, S. Study of quantitative and qualitative variations in essential oils of Sicilian oregano biotypes. *Journal of Essential Oil Research* **2015**, *27* (4), 293−306.
(47) Mancini, E.; Senatore, F.; Del Monte, D.; De Martino, L.; Grulova, D.; Scognamiglio, M.; Snoussi, M.; De Feo, V. Studies on chemical composition, antimicrobial and antioxidant activities of five Thymus vulgaris L. essential oils. *Molecules* **2015**, *20* (7), 12016−12028.
(48) Lee, S. J.; Umano, K.; Shibamoto, T.; Lee, K. G. Identification of volatile components in basil (Ocimum basilicum L.) and thyme leaves (Thymus vulgaris L.) and their antioxidant properties. *Food Chem.* **2005**, *91* (1), 131−137.
(49) Karapinar, M.; Esen Aktuğ, Ş. Inhibition of foodborne pathogens by thymol, eugenol, menthol and anethole. *Int. J. Food Microbiol.* **1987**, *4* (2), 161−166.
(50) Mendes, S. S.; Bomfim, R. R.; Jesus, H. C. R.; Alves, P. B.; Blank, A. F.; Estevam, C. S.; Antoniolli, A. R.; Thomazzi, S. M. Evaluation of the analgesic and anti-inflammatory effects of the essential oil of Lippia gracilis leaves. *Journal of Ethnopharmacology* **2010**, *129* (3), 391−397.
(51) Simon, J. E. Q. J.; Murray, J. G. Basil: A Source of Essential Oils. In *Advances in New Crops*; Janick, J., Simon, J. E., Eds.; Timber Press: Portland, OR, 1990; pp 484−489.
(52) Clinical and Laboratory Standards Institute. Performance standards for antimicrobial susceptibility testing; sixteenth informational supplement. CLSI document M100-S16CLSI, Wayne, PA; 2006.
(53) European Committee for Antimicrobial Susceptibility Testing (EUCAST) of the European Society of Clinical Microbiology and Infectious Diseases (ESCMID). Determination of minimum inhibitory concentrations (MICs) of antibacterial agents by broth dilution. *Clin. Microbiol. Infect.* **2003**, *9* (8), ix−xv.
(54) Wiegand, I.; Hilpert, K.; Hancock, R. E. Agar and broth dilution methods to determine the minimal inhibitory concentration (MIC) of antimicrobial substances. *Nat. Protoc* **2008**, *3* (2), 163−175.

https://doi.org/10.1021/acs.cgd.1c01435
Cryst. Growth Des. XXXX, XXX, XXX−XXX

(55) Sheldrick, G. M. SHELXT - integrated space-group and crystal-structure determination. *Acta Crystallogr. A Found. Adv.* **2015**, *71* (1), 3−8.
(56) Sheldrick, G. M. Crystal structure refinement with SHELXL. *Acta Crystallogr. C Struct. Chem.* **2015**, *71* (1), 3−8.
(57) Dolomanov, O. V.; Bourhis, L. J.; Gildea, R. J.; Howard, J. A. K.; Puschmann, H. OLEX2: a complete structure solution, refinement and analysis program. *J. Appl. Crystallogr.* **2009**, *42* (2), 339−341.
(58) Macrae, C. F.; Edgington, P. R.; McCabe, P.; Pidcock, E.; Shields, G. P.; Taylor, R.; Towler, M.; van De Streek, J. Mercury: visualization and analysis of crystal structures. *J. Appl. Crystallogr.* **2006**, *39*, 453−457.
(59) Kemperman, G. J.; de Gelder, R.; Dommerholt, F. J.; Raemakers-Franken, P. C.; Klunder, A. J. H.; Zwanenburg, B. Clathrate-Type Complexation of Cephalosporins with *β*-Naphthol. *Chem. - Eur. J.* **1999**, *5* (7), 2163−2168.
(60) Kemperman, G. J.; de Gelder, R.; Dommerholt, F. J.; Raemakers-Franken, P. C.; Klunder, A. J. H.; Zwanenburg, B. Induced fit phenomena in clathrate structures of cephalosporins. *Journal of the Chemical Society-Perkin Transactions 2* **2000**, No. 7, 1425−1429.
(61) Kemperman, G. J.; de Gelder, R.; Dommerholt, F. J.; Klunder, A. J. H.; Zwanenburg, B. Molecular selectivity and cooperativity in the clathrate-type complexation of cephradine. *Eur. J. Org. Chem.* **2002**, *2002* (2), 345−350.
(62) Groom, C. R.; Bruno, I. J.; Lightfoot, M. P.; Ward, S. C. The Cambridge Structural Database. *Acta Crystallogr. B Struct Sci. Cryst. Eng. Mater.* **2016**, *B72*, 171−179.
(63) Ropponen, H. K.; Richter, R.; Hirsch, A. K. H.; Lehr, C. M. Mastering the Gram-negative bacterial barrier - Chemical approaches to increase bacterial bioavailability of antibiotics. *Adv. Drug. Delivery Rev.* **2021**, *172*, 339−360.

https://doi.org/10.1021/acs.cgd.1c01435
Cryst. Growth Des. XXXX, XXX, XXX−XXX